*Protein Science* (2000), *9*:2322–2328. Cambridge University Press. Printed in the USA.


# Thermodynamic and structural characterization of Asn and Ala residues in the disallowed II′ region of the Ramachandran plot

M. CRISTINA VEGA,[1,3] JOSE C. MARTÍNEZ,[2,3] AND LUIS SERRANO[1]

[1]EMBL, Meyerhofstrasse 1, 69117 Heidelberg, Germany
[2]Departamento de Química Física, Facultad de Ciencias, Universidad de Granada, 18071-Granada, Spain

(RECEIVED June 6, 2000; FINAL REVISION September 22, 2000; ACCEPTED September 22, 2000)

**Abstract**

Residue Asn47 at position L1 of a type II′ $\beta$-turn of the $\alpha$-spectrin SH3 domain is located in a disallowed region of the Ramachandran plot ($\phi = 56 \pm 12$, $\psi = -118 \pm 17$). Therefore, it is expected that replacement of Asn47 by Gly should result in a considerable stabilization of the protein. Thermodynamic analysis of the N47G and N47A mutants shows that the change in free energy is small (~0.7 kcal/mol; ~3 kJ/mol) and comparable to that found when mutating a Gly to Ala in a $\alpha$-helix or $\beta$-sheet. X-ray structural analysis of these mutants shows that the conformation of the $\beta$-turn does not change upon mutation and, therefore, that there is no relaxation of the structure, nor is there any gain or loss of interactions that could explain the small energy change. Our results indicate that the energetic definition of II′ region of the Ramachandran plot ($\phi = 60 \pm 30$, $\psi = -115 \pm 15$) should be revised for at least Ala and Asn in structure validation and protein design.

**Keywords:** $\beta$-turn; protein design, Ramachandran plot, SH3 domain

The Ramachandran plot (Ramachandran & Sasisekharan, 1968) is a representation of the conformation of the main chain of a protein. It provides a convenient method for the analysis of the stereochemistry of the polypeptide chain backbone in protein structures, and it is an important guide of the overall correctness of a structure (Laskowski et al., 1996), immediately revealing any gross error in protein conformation. Additionally, the Ramachandran plot is key to the understanding of protein folding and stability and therefore provides guidance to protein design. Statistical studies on high-resolution structures show that there are still small but significant numbers of residues that remain in forbidden areas (Gunasekaran et al., 1996). Disallowed zones in the Ramachandran plot correspond to conformation distributions where steric clashes make protein folding energetically very expensive for all residues, or in some regions only for non-Gly residues. One of these areas is the so-called II′ zone ($\phi = 60 \pm 30$, $\psi = -115 \pm 30$), which is occupied by residues that are forming part of position L1 (following the nomenclature of Sibanda et al., 1989) in a type II′ beta-turn (Hutchinson & Thornton, 1994). This region in classical Ramachandran plots is only allowed for Gly, and, in fact, it is mainly this residue that occupies position L1 in type II′ turns (Wilmot & Thornton, 1988). However, it is evident that non-Gly residues are occasionally found in this area (Wilmot & Thornton, 1988; Jia et al., 1993; Stites et al., 1994; Gunasekaran et al., 1996; Ohage et al., 1997). An important question that remains to be answered is to what extent the occurrence of non-Gly residues in the II′ region results in a large conformational strain paid by the rest of the protein (Jia et al., 1993). Mutagenesis experiments changing a Gly into a Ala in the II′ region done in *Staphylococcal nuclease* (Stites et al., 1994) and the murine immunoglobulin light chain (Vk) (Ohage et al., 1997), resulted in small energy changes (5 and 2 kJ/mol, respectively). However, in these studies no three-dimensional (3D) structures for the mutants were provided; therefore, the possibility of a conformational rearrangement releasing the putative strain cannot be discarded. Yang et al. (1996), in a recent theoretical study using blocked dipeptides, calculated the difference in energy between Ala and Gly at position L1 of a type II′ $\beta$-turn, and concluded that it should be of the order of around ~5.4 kJ/mol. Thus, these studies suggests that at least Ala could be placed in the II′ region of the Ramachandran without a large energy penalty. To show that this is the case, we need to mutate a non-Gly residue in the II′ region by Ala and determine the 3D structure, as well as the effect on protein stability.

The $\alpha$-spectrin-SH3 domain (62 residues) folds into an orthogonal $\beta$-sandwich containing three $\beta$-hairpins (Fig. 1) and follows a two-state transition (Viguera et al., 1994). Of the three turns that are found in these domain, the last one (distal loop) is a regular

Reprint requests to: Luis Serrano, EMBL Structural Biology Program, Meyerhofstrasse 1, Heidelberg 69117, Germany; e-mail: Serrano@EMBL-Heidelberg.de.

[3]These authors have contributed equally to this work.

*Abbreviations:* CD, circular dichroism; DSC, differential scanning calorimetry; PCR, polymerase chain reaction; UV, ultraviolet; WT, wild-type.

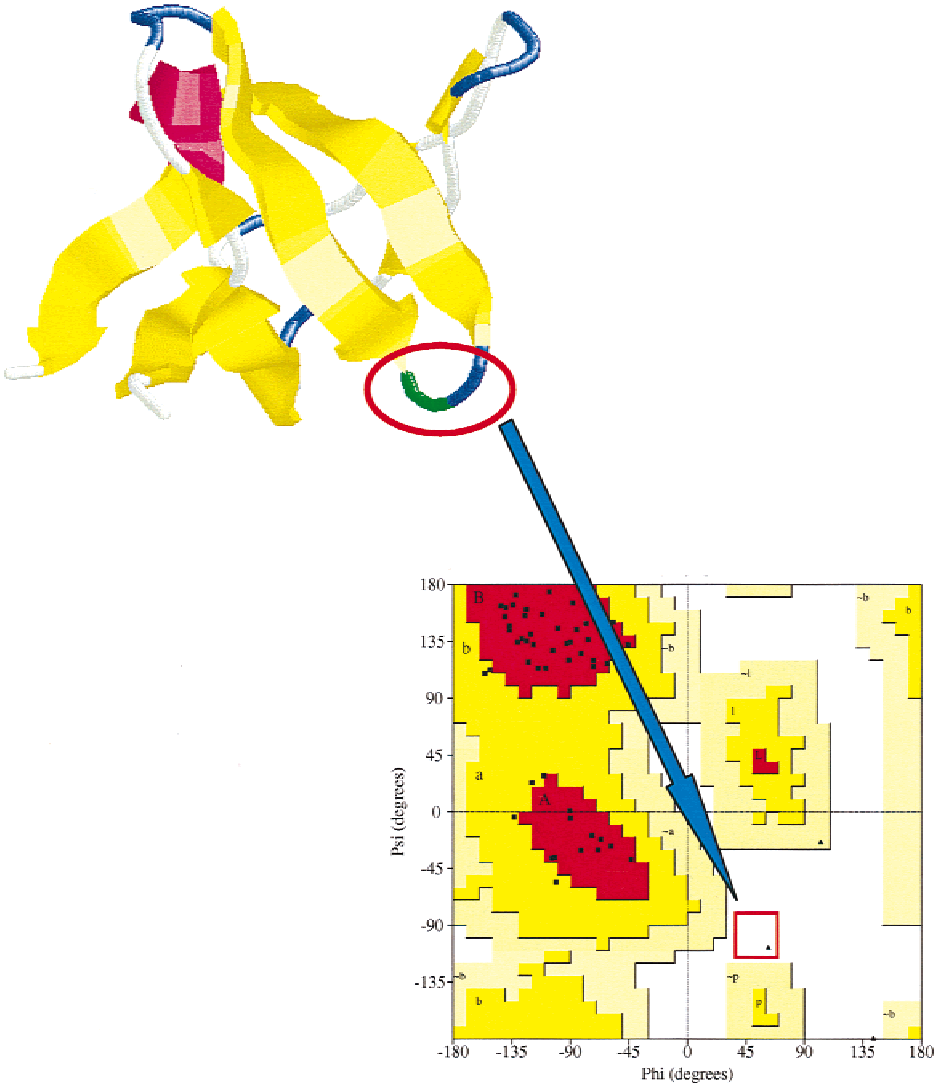


**Fig. 1.** Ribbon diagram of the $\alpha$-spectrin SH3 domain. Position 47 is shown in green. The arrow points to the II′ region of the Ramachandran plot in which this residue is found in the different structures of the WT and mutant SH3 domains.

type II′ beta-turn (Fig. 1) with the sequence Asn47–Asp48 at positions L1 and L2. Thus, residue Asn47 is placed in the II′ forbidden region of the Ramachandran plot. The location of Asn47 is not an artifact of the structure calculation, or due to crystal contacts, because it is found both in X-ray crystallography and NMR structures (Musacchio et al., 1992; Viguera et al., 1994) (Table 1).

In this work, to assess the importance of the conformational strain for non-Gly residues in the II′ zone, we have replaced Asn47 by Ala and Gly. The changes in protein stability, the effects in the kinetics of folding and unfolding, as well as the 3D structures of the two mutants have been determined.

## Results and discussion

### *Crystal structures*

The crystal structures of two $\alpha$-spectrin SH3 mutants: N47A and N47G have been solved at 2.0 and 1.8 Å resolution, respectively, by molecular replacement using the wild-type (WT) $\alpha$-spectrin SH3 structure (Viguera et al., 1995) as template. The packing in the crystals is similar to the packing of the WT domain. The crystals show one molecule by asymmetric unit with a Matthews coefficient of 2.4. Each molecule interacts with the symmetric related ones in the cell by hydrophobic contacts. The refined crystal structures of the N47G and N47A mutants (Table 2; Fig. 2) are similar to that of WT domain, and residues 47–48 adopt dihedral angles corresponding to a type II′ $\beta$-turn, as expected (Table 1). In all cases, the same number of main-chain hydrogen bonds and contacts in the $\beta$-turn are observed. Thus, any changes in stability can be solely ascribed to the introduction, or deletion, of side-chain groups and their interaction with the turn and the solvent.

### *Thermodynamic and kinetic analysis*

The kinetic analysis of the N47A mutant has been done at pH 7.0 and 3.0 (Fig. 3). The results of the analysis of the unfolding and

**Table 1.** *Dihedral angles from different structures in the distal loop of α-spectrin SH3 domain and free energy of unfolding ΔG at pH 7.0 for the WT and mutants at position 47 of the distal loop*[a]

| | Residue | | | | | | | | | | | | | | | | | |
|---|---|---|---|---|---|---|---|---|---|---|---|---|---|---|---|---|---|---|
| | 45 | | | 46 | | | 47 | | | 48 | | | 49 | | | 50 | | |
| | $\phi$ | $\psi$ | $\omega$ | $\phi$ | $\psi$ | $\omega$ | $\phi$ | $\psi$ | $\omega$ | $\phi$ | $\psi$ | $\omega$ | $\phi$ | $\psi$ | $\omega$ | $\phi$ | $\psi$ | $\omega$ |
| WT1 | −122 | 125 | −169 | −125 | 107 | −156 | 43 | −90 | −171 | −108 | −10 | −175 | −108 | 148 | 176 | −115 | 145 | 179 |
| WT2 | −117 | 153 | −177 | −114 | 104 | −172 | 57 | −101 | −176 | −118 | 13 | 177 | −129 | 147 | 174 | −172 | 145 | 179 |
| WT3 | −104 | 112 | 179 | −112 | 112 | −177 | 67 | −122 | 179 | −118 | 42 | −177 | −137 | 151 | 179 | −119 | 133 | −179 |
| WT4 | −86 | 115 | −171 | −142 | 128 | −179 | 66 | −72 | −175 | −150 | 11 | −162 | −144 | 140 | 173 | −97 | 92 | −167 |
| N47A | −121 | 118 | −179 | −109 | 112 | −176 | 57 | −122 | −178 | −110 | 34 | −178 | −123 | 147 | 179 | −130 | 150 | 179 |
| N47G | −124 | 119 | −179 | −111 | 111 | −179 | 67 | −108 | −177 | −119 | 22 | −177 | −137 | 146 | −177 | −106 | 170 | 179 |

[a]Dihedral angles of the backbone for the different distal loop conformations from α-spectrin SH3 domain structures available in literature: WT1 crystallographic structure at 1.8 Å (PDB code 1shg) (Musacchio et al., 1992); WT2 crystallographic structure of a pseudo-wild-type α-spectrin SH3 at 1.77 Å (PDB code 1pwt) (Viguera et al., 1994); WT3 NMR structure (PDB code 1aey) (Blanco et al., 1997); WT4 crystallographic structure of circular permutant in the residues 19–20 (PDB code 1tuc) (Viguera et al., 1993).

refolding reactions for this protein mutant are shown in Table 3. To obtain the kinetic and free energy parameters, we have fitted the folding and unfolding traces using a two-state model (see Materials and methods). The unfolding and refolding kinetic slopes, $m_{\ddagger\text{-}F}$ (related to the difference in solvent accessibility between the folded and transition states) and $m_{\ddagger\text{-}U}$ (between the unfolded and transition states), are similar within the experimental error to that previously described for the WT domain (Musacchio et al., 1992). Protein engineering analysis allows obtaining an estimate of the free energy contribution to the rate-limiting step in protein folding of the mutated group (Ferst & Serrano, 1993). This analysis permits to determine the so-called $\phi_{\ddagger}\text{-}U^{H_2O}$ value. This parameter measured for a mutant enables us to quantify the extent of interaction energy of the deleted group with the rest of the protein in the transition state ensemble, compared with the folded state (Ferst & Serrano, 1993). A value of $\phi_{\ddagger}\text{-}U^{H_2O} = 1$ indicates that the energy of a given interaction is the same in the transition state as in the folded state, and a null value indicates the absence of this interaction in the transition state. Intermediate $\phi_{\ddagger}\text{-}U^{H_2O}$ values correspond to partially formed interactions, or interactions fully formed within a fraction of the transition state ensemble.

In the case of the N47A protein and using the N47G protein as a reference (Martinez & Serrano, 1999), we find a very high value of $\phi_{\ddagger}\text{-}U^{H_2O}$ at both pHs, indicating that this region of the protein is almost fully folded in the transition state, as previously indicated based on other mutations (Martinez et al., 1998; Martinez & Serrano, 1999). However, this result is more conclusive because we show no conformational change upon mutation, and we are only deleting one methyl group (Ala vs. Gly).

The destabilization Gibbs energy induced by a mutation ($\Delta\Delta G_{F\text{-}U}$) has been calculated from the kinetic data and differential scanning calorimetry (DSC) (Table 4). At pH 7.0, the mutant N47A is 1.3 ± 0.2 kJ mol$^{-1}$ more unstable than the WT domain, while the mutant N47G is 1.7 ± 0.2 kJ mol$^{-1}$ more stable (Table 4). At low pH, the differences with the WT protein are somewhat different, probably due to the disruption of a possible pH dependent interaction of Asn47 with Asp48. However, the difference in energy between N47A and N47G (3.0 kJ mol$^{-1}$) is pH independent (Table 4). Similar results are obtained by differential DSC analysis of the proteins at pH 3.5 (Table 4). The DSC analysis shows a significant entropic change when mutating Asn47 to Gly, in part, compensated by the enthalpic component.

**Table 2.** *Refinement statistics for N47G and N47A mutants*

| | N47A | N47G |
|---|---|---|
| Resolution range (Å) | 8.0–2.0 | 8.0–1.8 |
| Number of reflections [$F_o > 2\sigma(F_o)$] | 3,485 | 5,796 |
| Total number of atoms (excluding hydrogens) | 349 | 543 |
| Number of solvent molecules | 44 | 70 |
| $R_{cryst}$ | 18.0 | 22.8 |
| $R_{free}$ | 25.5 | 28.0 |
| RMS deviations from target values | | |
| Bond lengths (Å) | 0.008 | 0.013 |
| Bond angles (deg) | 1.356 | 1.636 |

### *Protein structures database analysis*

The difference in free energy between the N47A and the N47G proteins is small and similar, but opposite in sign to that found between Ala and Gly in a α-helix (Martinez & Serrano, 1999). In agreement with this, statistical analysis of the protein structures database reveals that the differences in relative frequency of Gly and non-Gly residues in the II′ region of the Ramachandran plot (357 vs. 99 cases) is similar to that between other amino acids (excluding Pro) in the left-helical region. The average dihedral angle values for position L1 of the distal loop (located in the II′ region) in the SH3 protein domain structures used in our study is: $\phi = 56 \pm 12$, $\psi = -118 \pm 17$ (see Table 1). Searching in the protein structures database with this dihedral angle range (see Materials and methods) results in a proportionally larger number of non-Gly residues in this area (58 out of 122 cases). The small number of cases found is probably more related to the fact that this region is generally, although not always, associated to a type II′ β-turn, and it is not compatible with other regular secondary structure conformations. Interestingly enough, the number of non-Gly cases associated to a β-turn in the context of a β-hairpin is small (19%).

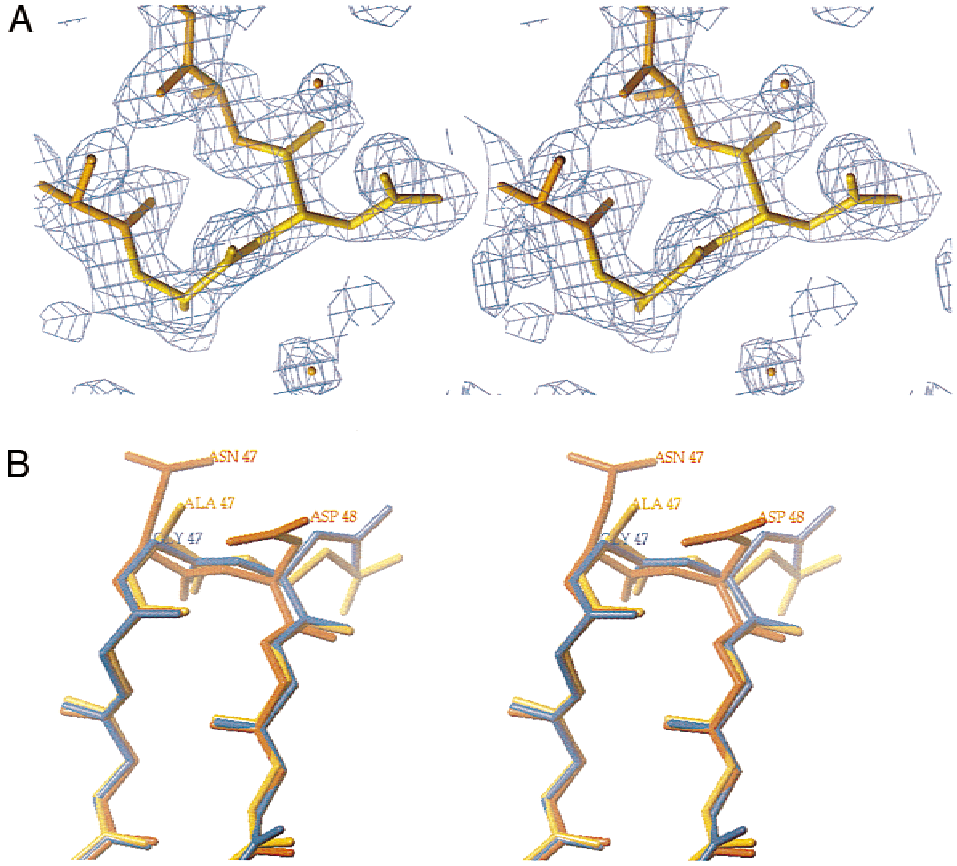


**Fig. 2.** Structure characterization of the mutants. **A:** Electron density map ($2F_o - F_c$) of the N47A mutant at $1\sigma$ level contour in the distal-loop. **B:** Stick model representation of the distal-loop crystal structure in the N47A (in yellow), N47G (in blue), and WT (in red, code, 1shg), spectrin $\alpha$-SH3 domain. The superimposition shows the conservation of the structure in the mutants at the II′ type beta-turn.

## Conclusion

The small changes in stability observed upon mutation of residue 47 to Gly or Ala are consistent with the experimental results obtained by other groups (Stites et al., 1994; Ohage et al., 1997), as well as close to the theoretical calculations done by Yang et al. (1996) using a model-blocked dipeptide. This small energy difference cannot be ascribed to a favorable contribution of the main-chain H-bond, because this interaction is present in the three proteins. Moreover, in the case of Ala, the side chain cannot make any significant electrostatic interactions with the polypeptide chain. Thus, the experimental values found in the spectrin-SH3 domain

**Table 3.** *Kinetic analysis of the N47A mutant at pH 7.0 and 3.5*[a]

| pH | $m_{\ddagger\text{-}F}$[b] (kJ mol$^{-1}$ M$^{-1}$) | $m_{\ddagger\text{-}U}$[c] (kJ mol$^{-1}$ M$^{-1}$) | $k_{\ddagger\text{-}F}$[d] ($s^{-1}$) | $k_{\ddagger\text{-}U}$[e] ($s^{-1}$) | $m_{F\text{-}U}$[f] (kJ mol$^{-1}$ M$^{-1}$) | $\Delta G_{F\text{-}U}$[g] | $\phi_{\ddagger\text{-}U}$[h] (kJ mol$^{-1}$) |
|---|---|---|---|---|---|---|---|
| 3.5 | −2.51 ± 0.09 | 5.2 ± 0.1 | 0.027 ± 0.002 | 3.3 ± 0.2 | 7.7 | 11.9 | 1.3 ± 0.2 |
| 7.0 | −1.80 ± 0.09 | 4.3 ± 0.09 | 0.0055 ± 0.0007 | 2.05 ± 0.0 | 86.1 | 14.6 | 0.8 ± 0.2 |

[a] The experimental conditions and analysis are described in Materials and methods. The errors shown correspond to the fitting errors.
[b] Dependence of the natural logarithm of unfolding with urea.
[c] Dependence of the natural logarithm of refolding with urea.
[d] $k_{\ddagger\text{-}F}$, unfolding rate constant in water.
[e] Refolding rate constant in water.
[f] Dependence of the natural logarithm of the equilibrium constant with urea, obtained from the kinetic parameters $m_{\ddagger\text{-}F}$ and $m_{\ddagger\text{-}U}$.
[g] Dependence of the Gibbs energy of unfolding with urea (Gibbs energy of unfolding of the mutants determined from the kinetic parameters).
[h] Phi values for refolding using the N47G mutant as in Martinez and Serrano (1999).

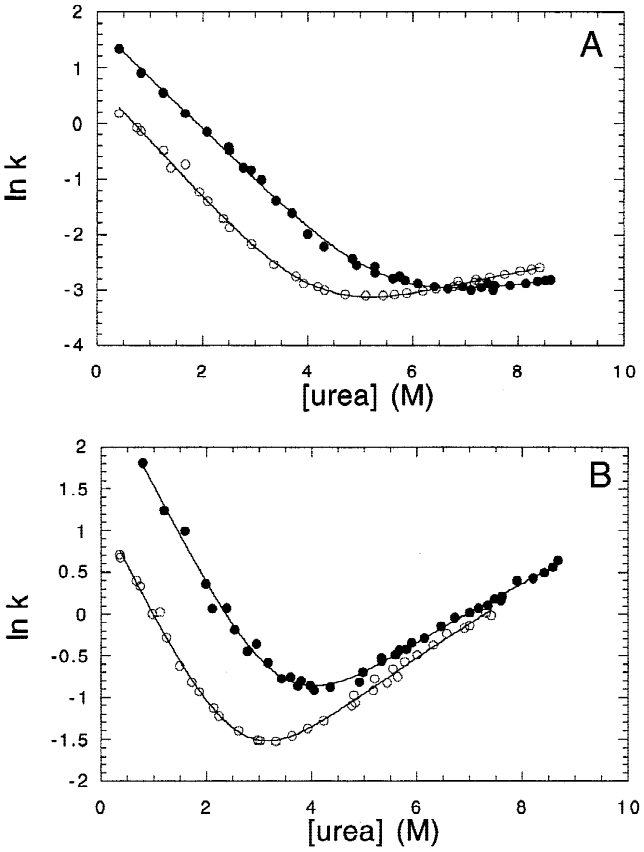


**Fig. 3.** Kinetic analysis in folding and unfolding reaction of the mutants N47G and N47A at pH = 3.5 and 7.0. (Empty circles) N47A data, (filled circles) N47G data: (**A**) pH 3.5, (**B**) pH 7.0. The solid lines represent the best fit of the whole data set to Equation 2 described in Materials and methods.

are not system, or context dependent, but rather reflect a general result. The observed change in stability is comparable to that found in $\alpha$-helices when mutating an Ala to Gly. This means that at least Ala and Asn can be placed in the II′ region of the Ramachandran plot with a small energy cost. Similarly, they do not induce a high increase in the energy barrier in the protein folding.

In addition, on the basis of our results and taking into account the earlier theoretical and experimental works, the II′ region of the Ramachandran plot should be considered for some residues as an allowed region from an energetic point of view. Our results do not change the topography of the Ramachandran Plot, but they highlight the fact that the zone II′ on the Ramachandran Plot should be considered energetically allowed at least for Asn and Ala. The results presented here are important for protein structure calculation and protein design of $\beta$-turns, and should be taken into account, for instance, during structure validation process.

## Materials and methods

### *Protein database search*

The database of 3D structures has been obtained following the principles described by Hobohm et al. (1992). This database has been filtered for quality of the data and consists of 279 proteins with less than 25% sequence homology for a total of 59,117 amino acidic residues (the list of proteins is shown in Munoz & Serrano, 1995), and it is currently included in the program WHATIF (Vriend, 1990). The search was conducted using the Scan3D option, and the search query was done using the $\phi$-$\psi$ suboption.

### *Mutagenesis and purification*

The mutants, obtained by the polymerase chain reaction (PCR) method (Higuchi et al., 1988), were expressed and purified as previously indicated (Viguera et al., 1994). Protein concentration was determined using the method of Gill and von Hippel (1989) to obtain the extinction coefficient, that was 2.26 mL/cm mg.

### *Kinetic measurements*

Folding and unfolding kinetics were followed in a biologic stopped-flow machine by fluorescence emission selected with a 305 nm

**Table 4.** *Thermodynamic parameters for the WT and mutant proteins at pH 7.0 and 3.5*[a]

| Chemical | Protein | $m_{\ddagger-U}$ (kJ mol$^{-1}$ M$^{-1}$) | $\Delta G_{F-U}$ (kJ mol$^{-1}$) | $\Delta\Delta G_{F-U}$ (kJ mol$^{-1}$) |
|---|---|---|---|---|
| pH 7.0 | WT* | −5.5 ± 0.2 | 15.9 ± 0.1 | |
| | N47G* | −5.6 ± 0.1* | 17.6 ± 0.1 | −1.7 |
| | N47A | −6.1 ± 0.1* | 14.6 ± 0.1 | 1.3 |
| pH 3.5 | WT* | −7.6 ± 0.2 | 12.5 ± 0.1 | |
| | N47G* | −7.6 ± 0.2 | 15.0 ± 0.2 | −2.5 |
| | N47A | −7.7 ± 0.1 | 11.3 ± 0.1 | 1.2 |

| Calorimetry | Protein | $T_m$ (K) | $\Delta C_{p,U}(T_m)$ (kJ K$^{-1}$ mol$^{-1}$) | $\Delta H_U\ (T_m)$ (kJ mol$^{-1}$) | $\Delta S_U(298)$ (J K$^{-1}$ mol$^{-1}$) | $\Delta G_U(298)$ (kJ mol$^{-1}$) | $\Delta\Delta G_{F-U}$ (kJ mol$^{-1}$) |
|---|---|---|---|---|---|---|---|
| pH 3.5 | WT | 336.0 | 2.9 | 188 | 155 | 13.9 | |
| | N47G | 339.1 | 2.1 | 197 | 185 | 16.0 | −2.1 |
| | N47A | 333.9 | 3.2 | 193 | 145 | 13.4 | 0.5 |

[a]The errors in experimental values of $\Delta H_m$ and $\Delta C_{p,U}(T_m)$ are about 8%, 20% for $\Delta G_U(298)$ and around 0.7 K for $T_m$.
[b]Data taken from Viguera et al. (1994) and Martinez and Serrano (1999).

cutoff filter upon excitation at 290 nm. The buffer used was 50 mM sodium phosphate pH 7.0 or 50 mM glycine/HCl pH 3.5. The cell chamber and the syringes were kept at 298 K. In the SH3 domain, there are two Trp (41 and 42). The fluorescence and far-UV CD traces have been shown to be identical (Viguera et al., 1994). The kinetic phases have been fitted to mono-exponential by means of algorithms provided by Biologic Software from where *k*, the rate constant at a given concentration of denaturant, was calculated. The *cis-trans* Pro isomerization slow refolding phase is not considered in this analysis.

### *Determination of the kinetic and thermodynamic parameters*

When studying the unfolding and refolding reactions of unstable SH3 mutants, it has been found that the changes in the natural logarithm of the unfolding rate constant with urea are not linear and curve at high urea concentrations (Viguera et al., 1994). A similar phenomenon has been described for barnase (Johnson & Fersht, 1995).

In SH3 domain, fitting of several of these unstable mutants has shown that the curvature of the unfolding data follows the next equation (which also reproduces the data in barnase):

$$\ln k_{\ddagger\text{-}F}([\text{urea}]) = \ln k_{\ddagger\text{-}F} + m_{\ddagger\text{-}F}[\text{urea}] - 0.014[\text{urea}]^2. \quad (1)$$

Accordingly, the kinetic data were fitted to the equation:

$$\ln k([\text{urea}]) = \ln(k_{\ddagger\text{-}U} \exp(m_{\ddagger\text{-}U}[\text{urea}]) + k_{\ddagger\text{-}F} \exp(m_{\ddagger\text{-}F}[\text{urea}] - 0.014\,[\text{urea}]^2)) \quad (2)$$

where $k_{\ddagger\text{-}U}$ and $k_{\ddagger\text{-}F}$ are the refolding and unfolding rate constants in water, respectively. $m_{\ddagger\text{-}U}$ and $m_{\ddagger\text{-}F}$ are the slopes of ln *k* vs. [urea] in the refolding and unfolding reactions, respectively. The equilibrium free energy of unfolding can be calculated from the $k_{\ddagger\text{-}U}$ and $k_{\ddagger\text{-}F}$ values:

$$\Delta G_{F\text{-}U} = -RT(\ln(k_{\ddagger\text{-}U}) - \ln(k_{\ddagger\text{-}F})). \quad (3)$$

Calculation of the Gibbs energy of unfolding, using a nonlinear term in the unfolding reaction, produces a good agreement with the calorimetric data (Prieto et al., 1997), as it happened with barnase (Johnson & Fersht, 1995).

### *Differential scanning calorimetry (DSC)*

Calorimetric experiments were performed with the computerized version of the DASM-4 microcalorimeter (Biopribor, Puschino, Russia) with platinum cells of 0.47 mL volume at 1 and 2 K/min. Before being placed in the cell, the samples were extensively dialyzed against buffers with the appropriate pH. Because the experiments were conducted between pH 2 and 4, buffers were either 50 mM glycine/HCl or 50 mM acetic acid/sodium acetate. The concentration of the protein in calorimetric experiments was between 2 and 6 mg/mL. The samples were routinely heated up to 383 K and then cooled slowly inside the calorimeter and reheated once again to check the reversibility of the unfolding. Signals recovered 80% of their initial amplitude in all experiments, depending on the exposure of the sample to high temperature. The calorimetric records were transformed into the temperature dependencies of the partial molar heat capacity and analyzed as described elsewhere (Martinez & Serrano, 1999) and below.

To fit the data, we followed the two-state model, using a nonlinear $C_{p,U}$ function in the same way as for WT domain (Viguera et al., 1994). Moreover, we have performed a direct global fitting of all the curves to the model to get a unique and more reliable $\Delta C_{p,U}(T)$ function. The expression we obtained was

$$\Delta C_{p,U}(T) = -2.39 + 0.076T - 0.0001795T^2 \text{ (kJ/K mol)}. \quad (4)$$

The enthalpy values we obtained from the fitting (Table 4) follow, between the limits of error, the WT $\Delta H_U(T_m)$ vs. $T_m$ correlation (data not shown).

### *X-ray crystallography*

Single crystals of the N47G and N47A mutants of $\alpha$-spectrin SH3 protein domain were grown as described previously for WT (Viguera et al., 1994). Diffraction patterns were collected using Hamburg synchrotron radiation at the DORYS storage ring. The data sets were processed with DENZO, scaled and merged with SCALEPACK (Otwinosky, 1993) with an *R*-merge of 3.7 and 7.5%, respectively, with completeness of 75 and 93% in the shell of highest resolution for mutant N47G and N47A, respectively. The coordinates from WT $\alpha$-spectrin SH3 domain (Protein Data Bank (PDB) code 1shg) were used as starting model for both mutant structure determinations using the AMoRe program (Navaza, 1994). The final solution for both mutants were found using the $F_{obs}$ between 12–2.5 Å and shows a correlation coefficient of 0.69 and a *R*-factor of 0.40 for the N47G mutant and a correlation factor of 0.59 and an *R*-factor of 0.40 for the N47A mutant. The refinement was performed with an X-PLOR package (Brünger, 1992a, 1992b). During the refinement, the $2F_o - F_c$ and $F_o - F_c$ electronic density maps were displayed with the graphic program TURBO (Cambillau & Horjales, 1987). The turn is clearly defined by the electronic density map ($2F_o - F_c$) at the $1\sigma$ level. The final coordinates have been submitted to the Protein Data Bank (EBI) with codes 1qkw (N47G) and 1qkx (N47A).

## Acknowledgments

M.C.V. and J.C.M. acknowledge E.U. for their TMR potsdoctoral fellowship, Prof. P.L. Mateo for the generous offer of calorimetric techniques, A. González and F.J. Fernández for their help and interest at EMBL-Outstation in DESY Hamburg, and M. Pethukov for his great interest and helpful discussions. The first two authors have contributed equally to this work.

This work was partly supported by EU Network FMRX-CT96-0013, EU Grant B104-CT972180 and MCC project PB96-1446.

## References

Blanco FJ, Ortiz AR, Serrano L. 1997. $^1$H and $^{15}$N assignment and solution structure of the SH3 domain of spectrin: Comparison of unrefined and refined structure sets with the crystal structure. *J Biomol NMR 9*:347–357.

Brünger AT. 1992a. *X-PLOR, version 3.1*. New Haven, Connecticut: Yale University Press.

Brünger AT. 1992b. Free R-value: A novel statistical quantity for assessing of crystal structure. *Nature 355*:472–475.

Cambillau C, Horjales E. 1987. TOM, a FRODO a subpackage for protein and ligand fitting with interactive energy minimization. *J Mol Graphics 5*:174–177.

Ferst A, Serrano L. 1993. Principles of protein stability from protein engineering experiment. *Curr Opin Struct Biol 3*:75–78.

Gill SJ, von Hippel PH. 1989. Calculation of protein extinction coefficients from amino acid sequence data. *Anal Biochem 182*:319–326.

Gunasekaran K, Ramakrishnan C, Balaram P. 1996. Disallowed Ramachandran conformations of amino acid residues in protein structures. *J Mol Biol 264*:191–198.

Higuchi R, Krummel B, Saiki RK. 1988. A general method of *in vitro* preparation and specific mutagenesis of DNA fragments: Study of protein and DNA interactions. *Nucleic Acids Res 16*:7351–7367.

Hobohm U, Scharf M, Schneider R, Sander C. 1992. Selection of representative protein data sets. *Protein Sci 1*:409–417.

Hutchinson EG, Thornton JM. 1994. A revised set of potentials for $\beta$-turn formation in proteins. *Protein Sci 3*:2207–2216.

Jia Z, Quail JW, Waygood EB, Delbaere LT. 1993. Active-centre torsion-angle strain revealed in 1.6 A-resolution structure of histidine-containing phosphocarrier protein. *J Biol Chem 268*:22490–22501.

Johnson CM, Fersht AR. 1995. Protein stability as a function of denaturant concentration: The thermal stability of barnase in the presence of urea. *Biochemistry 34*:6795–6804.

Laskowski RA, Rullmannn JA, MacArthur MW, Kaptein R, Thornton JM. 1996. AQUA and PROCHECK-NMR: Programs for checking the quality of protein structures solved by NMR. *J Biomol NMR 8*:477–486.

Martinez JC, Pisabarro MT, Serrano L. 1998. Obligatory steps in protein folding and the conformational diversity of the transition state. *Nat Struct Biol 5*:721–729.

Martinez JC, Serrano L. 1999. The folding transition state between SH3 domains is conformationally restricted and evolutionarily conserved. *Nat Struct Biol 6*:1010–1016.

Munoz V, Serrano L. 1995. Intrinsic secondary structure propensities of the amino acids, using statistical $\phi$-$\psi$ matrices: Comparison with the experimental scales. *J Mol Biol 245*:275–296.

Musacchio A, Noble M, Pauptit R, Wierenga R, Saraste M. 1992. Crystal structure of a src-homology 3 (SH3) domain. *Nature 359*:851–855.

Navaza J. 1994. AmoRe an automated package for molecular replacement. *Acta Crystallogr A50*:157–163.

Ohage EC, Graml W, Walter MM, Steinbacher S, Steipe B. 1997. Beta-turn propensities as paradigms for the analysis of structural motifs to engineer protein stability. *Protein Sci 6*:233–241.

Otwinosky Z. 1993. *Proceedings of the CCP4 study weekend: Data collection and processing*. Daresbury, U.K.: Daresbury Laboratory.

Prieto J, Wilmans M, Jimenez MA, Rico M, Serrano L. 1997. Non-native local interactions in protein folding and stability: Introducing a helical tendency in the all $\beta$-sheet $\alpha$-spectrin SH3 domain. *J Mol Biol 268*:760–778.

Ramachandran GN, Sasisekharan V. 1968. Conformation of polypeptides and proteins. *Adv Protein Chem 23*:283–438.

Sibanda BL, Blundell TL, Thornton JM. 1989. Conformation of beta-hairpins in protein structures. A systematic classification with applications to modelling by homology, electron density fitting and protein engineering. *J Mol Biol 206*:759–777.

Stites WE, Meeker AK, Shortle D. 1994. Evidence for strained interactions between side-chains and the polypeptide backbone. *J Mol Biol 235*: 27–32.

Viguera AR, Blanco FJ, Serrano L. 1995. The order of secondary structure elements does not determine the structure of a protein but does affect its folding kinetics. *J Mol Biol 247*:670–681.

Viguera AR, Martinez JC, Filimonov VV, Mateo PL, Serrano L. 1994. Thermodynamic and kinetic analysis of the SH3 domain of spectrin shows a two-state folding transition. *Biochemistry 33*:2142–2150.

Vriend G. 1990. WHATIF: A molecular modeling and drug design program. *J Mol Graph 8*:52, 29.

Wilmot CM, Thornton JM. 1988. Analysis and prediction of the different types of b-turns in proteins. *J Mol Biol 203*:221–232.

Yang A-S, Benjamin H, Honig B. 1996. Free energy determinants of secondary structure formation: III. $\beta$-Turns and their role in protein folding. *J Mol Biol 259*:873–882.